Fixed time controller for police quadcopter aircraft based on integral backstepping method

Xiaolong Tian [*] **Qiwei Sun** [*] **Nan Wang** [**]

[*] *School of Urban Rail Policing, Zhengzhou Police University, Nongye Road, Zhengzhou, 450053, Henan Province, China(e-mail: xintianlinglong@163.com, 18814105698@163.com)*
[**] *College of Information Engineering, Henan University of Science and Technology, Kaiyuan Street, Luoyang, 471000, Henan Province, China(e-mail: wswn2019@163.com)*

Abstract: To enhance the trajectory tracking response speed of police quadcopter drones and simplify engineering implementation, this paper proposes a fixed-time attitude tracking control strategy based on the backstepping integration method. The approach integrates fixed-time control theory to achieve rapid and effective tracking of the aircraft's position and attitude within a predefined time, ensuring the stability of the quadcopter flight controller. Additionally, the aircraft model characteristics are analyzed, and an integral term is incorporated into the backstepping-based attitude fixed-time control design. By selecting appropriate constants for the integral term, the control law is simplified, improving the practicality of the control algorithm. Compared to PID controller, the proposed method reduces the error in the x-direction by 50% and in the y-direction by 80%. When compared to sliding mode controller, the x-direction error is reduced by 2%, and the y-direction error decreases by 60%. The yaw angle error under the proposed controller is nearly zero. Furthermore, compared to the backstepping controller without the integral term, the proposed controller reduces the computational time per step by 51.6%. Simulation results demonstrate that the proposed controller achieves faster and more stable trajectory tracking compared to both PID and sliding mode controllers.

Keywords: Quadcopter aircraft, fixed time control, integral backstepping method, trajectory tracking.

1. INTRODUCTION

With its flexibility and maneuverability, quadrotor UAVs can swiftly patrol railway lines, particularly in areas with complex terrain and hard-to-reach spots, such as mountains and riverbanks (Maghazei et al., 2020). This allows them to promptly identify potential safety hazards on the railway, such as damaged protective fences or illegal trespassing. Additionally, by carrying high-definition cameras and sensors, quadrotor UAVs can monitor railway conditions in real-time, providing railway police with intuitive on-site footage, which aids in the timely response and handling of emergencies. These tasks inevitably involve the tracking of quadrotor UAVs (Askarzadeh et al., 2023). Simultaneously, the uncertainty of their model parameters and the strong coupling of nonlinearity pose significant challenges to the rapid stability control of quadrotor aircraft (Fox et al., 2020).

⋆ This work was supported in part by the Scientific and Technological Project of Henan Province under Grant (252102241051), the Open Project Program of the State Key Laboratory under Grant (RGZNYGGAO-2412), the Fundamental Research Funds for Central Universities (Grant Nos.2025TJJBKY009, 2025TJJBKY023, 2025TJJBKY006, 2025TJJBKY021).
Corresponding author:Qiwei Sun, E-mail: 18814105698@163.com.

The control algorithm is the core of UAV trajectory tracking. Common algorithms include PID control, sliding mode control, backstepping control, and more. Ameret et al. (Amertet et al., 2024) designed a hybrid fuzzy PID controller to manage the state of the quadcopter (rolling, altitude, and airspeed), integrating it into the intelligent agriculture system to significantly enhance agricultural production efficiency. PID control adjusts the three parameters of proportion, integration, and differentiation to regulate the flight attitude and speed of the UAV (Ezhil et al., 2022). However, in the face of complex environments and parameter variations, PID control often struggles to meet precision and robustness requirements. To enhance the system's robustness, Liu et al. (Liu et al., 2024) proposed a double closed-loop active disturbance rejection sliding mode control scheme for the tilted quadcopter, which exhibits nonlinearity, strong coupling, and sensitivity to interference, to facilitate target trajectory tracking. The sliding mode manifold control law for the tilted quadcopter was designed using the hyperbolic tangent sliding mode control method. Sliding mode control exhibits the ability to disregard external disturbances and uncertain parameters. By establishing suitable switching conditions on the sliding mode surface, the system gains immunity to external disturbances and uncertainties (Ullah et al., 2019). This makes sliding mode control have significant advantages in dealing with UAV flight systems with large uncertainties and disturbances. In order to improve the robustness of altitude control, Smith et al. (Smith et al., 2024) proposed a new high-order sliding mode observer (HOSMO) adaptive gain selection technique, which combines the disturbance observer with the super-twisting sliding mode controller to effectively attenuate the chattering phenomenon. Considering the interference and model uncertainty, Ahn et al. (Ahn et al., 2023) designed a sliding mode controller using adaptive approach laws and super-twisting algorithms to improve the sliding mode control and stability of UAV flight. The use of the super-twist algorithm overcomes the discontinuous signal of traditional strategies, effectively improving the response speed and robustness of the system. Nevertheless, a well - known drawback of sliding mode control is the chattering phenomenon, which commonly occurs during the switching of the sliding mode surface (Labbadi et al., 2021). This chattering, manifested as high - frequency oscillations in the control input, can excite unmodeled high - frequency dynamics in the system. In extreme cases, these excited high - frequency dynamics can lead to instability of the overall control system, potentially causing it to collapse. Despite numerous proposed solutions, chattering persists as a hurdle in the practical deployment of sliding mode control. Alternatively, backstepping control offers notable flexibility and reduced hardware demands. In contrast to sliding mode control, backstepping control boasts systematic and structured design approaches, applicability to intricate nonlinear systems, superior transient performance, and inherent robustness. At the same time, the problems of chattering, design complexity, and high hardware requirements in sliding mode control have been better solved in backstepping control (Sartori et al., 2021). Belmouhoub et al. (Belmouhoub et al., 2023) proposed a backstepping controller based on finite-time Lyapunov stability theory and enhanced by the hyper-twist algorithm to solve the trajectory tracking problem of non-traditional quadrotor aircraft with rotating arms (also known as foldable drones). The findings indicate that the introduced control strategy exhibits excellent performance in both accuracy and stability. Due to the change of UAV geometric parameters with time, Derrouaoui et al. (Derrouaoui et al., 2022) proposed an efficient nonlinear adaptive integral inversion controller. The control framework incorporates estimators for inertia and dedicated modules for computing the center of gravity and mixing matrix. A comparison of the proposed control approach with traditional integral inversion controllers, both in undisturbed and disturbed scenarios, demonstrates enhanced system robustness. Jahan et al. (Jahan et al., 2024) designed a new type of firefighting drone based on adaptive optimization technology of fuzzy inverse control. The drone's anticipated position and altitude are tightly controlled, enabling precise data monitoring, including real-time imaging, gas concentration measurements, and fire location detection, thereby mitigating risks for firefighters and furnishing crucial information for firefighting efforts.

The control strategies described above are mainly designed to achieve asymptotic tracking control. In an asymptotic tracking scenario, the tracking error converges to zero as time approaches infinity (Zheng et al., 2024). However, in many practical applications, such as railway patrol and emergency response using quadrotor UAVs, rapid tracking is of utmost importance. The slow convergence inherent in asymptotic tracking may not be able to meet the real - time requirements of these applications, where timely detection and response to events are critical. Consequently, several finite-time trajectory tracking control strategies have been developed (Ghommam et al., 2020; Jammazi et al., 2021; Wang et al., 2017; Eliker et al., 2021; Liu et al., 2021). Ghommam et al. (Ghommam et al., 2020) proposed a leader-follower synchronization technique for unmanned aerial vehicle (UAV) rendezvous, designing a finite-time tracking control algorithm via output feedback for the follower UAV while ensuring that the input constraints of the UAV are satisfied. This approach overcomes the challenges posed by the underactuated nature of UAVs, enabling the tracking error of the closed-loop system to converge within a finite time. Jammazi et al. (Jammazi et al., 2021) discussed the extension of several sufficient conditions for finite-time stability and applied them to the attitude tracking system of the UAV X4, with simulation results indicating a significant improvement in trajectory tracking speed. Eliker et al. (Eliker et al., 2021) proposed a non-singular finite-time adaptive robust controller for quadrotors based on inverse command filtering and non-singular fast terminal sliding mode control. This method uses a small number of adaptive laws to estimate parameters and non-parametric uncertainties, alleviating the chattering phenomenon and satisfying practical finite-time stability. This paper investigates the tracking control problem of a tilting quadrotor with unknown nonlinearities. Liu et al. (Liu et al., 2021) combined neural networks with finite-time control to propose an adaptive finite-time neural control for tilting quadrotors, where all tracking errors and estimation errors can converge to a small neighborhood near zero within a finite time, effectively solving the trajectory tracking challenge of tilting quadrotors.

For traditional finite - time control algorithms, the estimation of convergence time is highly dependent on the initial conditions of the system (Kangunde et al., 2021). Mathematically, different initial states of the system will lead to different convergence times, which limits their predictability in practical applications. In sharp contrast, fixed - time control algorithms offer a significant advantage in that their performance is independent of the initial conditions of the system (Zhang et al., 2023; Ning et al., 2022). The user can pre - define the upper bound of the convergence time, regardless of the initial states of the system, providing a more reliable and consistent control performance. Cheng et al. (Cheng et al., 2022) introduced a novel nonsingular fixed-time sliding mode control technique that provides fixed-time position and attitude tracking control for quadrotors, enabling a more accurate determination of convergence time. In contrast to finite-time tracking control, the proposed strategy guarantees that the convergence time's upper limit is unaffected by the system's initial conditions. Considering the underactuated characteristics and external disturbances of the quadrotor suspension transport system, Liu et al. (Liu et al., 2022) developed an adaptive hierarchical sliding mode control scheme based on fixed-time sliding mode disturbance observers for underactuated quadrotor systems. This approach utilizes adaptive laws to address disturbance estimation errors, and experimental results demonstrate the effectiveness and potential of fixed-time control technology.

Consequently, despite significant advancements in aircraft control, several issues persist in practical applications, including the complexity of controller algorithms and the difficulty of their physical implementation, as well as the challenges associated with achieving precise control over convergence speed using conventional methods. To address these challenges, we designed a fixed-time controller for quadrotors based on the integral backstepping method. This controller not only simplifies the algorithm but also facilitates rapid tracking control within a fixed time frame. The main contributions of this work are as follows:

(1) In the control design process, an integral term was introduced into the backstepping method for attitude control. By selecting appropriate constants for the integral term, the controller model was simplified, enhancing the practicality of the algorithm and reducing the execution time of the model. Simulation experiments demonstrated that this controller can achieve error-free trajectory tracking.
(2) By integrating backstepping methods with fixed-time control, a fast and stable controller for the aircraft was developed. The smoothness of the proposed control law effectively mitigates issues related to controller chattering and the singularity of the derivatives of the virtual control signals.
(3) Utilizing Lyapunov stability theory, the proposed controller guarantees that the tracking error converges to a small vicinity of the origin within a specified timeframe, ensuring boundedness of all closed-loop signals. Numerical simulations comparing the proposed controller with PID and sliding mode controls highlight its substantial advantages in terms of swift convergence and stability.

2. PRELIMINARY KNOWLEDGE

The stability of the system is the most basic problem in the field of control research. Lyapunov stability is one of the most important theories in the stability theory of control science. Among them, the second Lyapunov theorem is the most widely used. It abstracts the Lyapunov function with the characteristics of system energy from the characteristics of system energy function, which makes it easier to judge and prove the stability. The fixed time control is based on this theoretical framework. By designing a specific form of Lyapunov function and constraining the convergence rate of its derivative, the system state is stable in a fixed time. The quadrotor aircraft studied in this paper is an underactuated rigid body with four inputs and six outputs. By establishing the system equation with six state variables (six variables are the position variables (x, y, z) describing the space position of the aircraft and the attitude variables (ϕ, θ, ψ) describing the attitude position of the aircraft), the flight controller is designed using the fixed time control method. Therefore, the following two theorems are mainly used to complete the controller design.

Lemma 1 (Wang et al., 2021): For a nonlinear system $\dot{x} = f(t, x)$, $x(t_0) = x_0$, $f(0)$ is uniformly ultimately bounded within t, and there exists a positive definite function $V(x)$, whose derivative satisfies the following:

$$\dot{V}(x) \leq -\sigma V(x)^{\upsilon_1} - \delta V(x)^{\upsilon_2} \tag{1}$$

where $\sigma > 0, \delta > 0, 0 < \upsilon_1 < 1, \upsilon_2 > 1$, then the origin of the system is globally fixed time stable and the settling time function T can be estimated by

$$T \leq T_{\max} := \frac{1}{\sigma(1-\upsilon_1)} + \frac{1}{\delta(\upsilon_2 - 1)} \tag{2}$$

Furthermore, if $\upsilon_1 = 1 - \frac{1}{\upsilon_3}$and $\upsilon_2 = 1 + \frac{1}{\upsilon_3}$ with $\upsilon_3 > 1$ are selected, the settling time function T can be estimated by a less conservative bound

$$T_{\max} := \frac{\pi \upsilon_3}{2\sqrt{\sigma\delta}} \tag{3}$$

Lemma 2 (Wang et al., 2023): For any $j_{i(1\ldots n)} > 0$, the following inequality holds:

$$(\sum_{i=1}^{n} j_i)^2 \leq n \sum_{i=1}^{n} j_i^2 \tag{4}$$

3. QUADROTOR MODEL

Figure 1 is the schematic diagram of inertial coordinate system and body coordinate system of quadrotor aircraft. The aircraft has four mutually independent motors to drive their respective propellers to rotate. Propellers 1 and 3 rotate counterclockwise, while propellers 2 and 4 rotate clockwise. By controlling the speed of each propeller, the flight attitude of the aircraft can be changed. The quadrotor aircraft has a total of six degrees of freedom, which describes the rectangular coordinate system (x, y, z)?and the attitude angles (ϕ, θ, ψ) that describe the flight mode of the aircraft. The system model establishes the inertial coordinate system and the coordinate system of the body itself, and represents the flight attitude of the aircraft through mutual transformation. Firstly, the pre-designed inertial coordinate system is coincided with the origin of the object coordinate system, and then the Euler angle is used to represent the angle between the coordinates corresponding to the inertial coordinate system and the object coordinate system. The three attitude angles of the aircraft are roll angle ϕ, pitch angle θ and yaw angle ψ . Among them, the value range of roll angle and pitch angle is $(-\pi/2, \pi/2)$, and the value range of yaw angle is $(-\pi, \pi)$. The control input quantity of quadrotor aircraft is (u_1, u_2, u_3, u_4), where u_1 represents the input control quantity in the vertical direction of the aircraft; u_2 is the input control quantity of aircraft roll angle; u_3 is the input control value of aircraft pitch angle; u_4 represents the input control quantity of aircraft yaw angle. The input variable expression of quadrotor UAV is as follows:

$$\begin{cases} u_1 = F_1 + F_2 + F_3 + F_4 \\ u_2 = (F_4 - F_2)l \\ u_3 = (F_3 - F_1)l \\ u_4 = (F_4 + F_2 - F_1 - F_3)l \end{cases} \tag{5}$$

where, l is the distance between the rotor and the centroid of the UAV, and $F_i (i = 1, 2, 3, 4)$ is the lift generated by each motor.

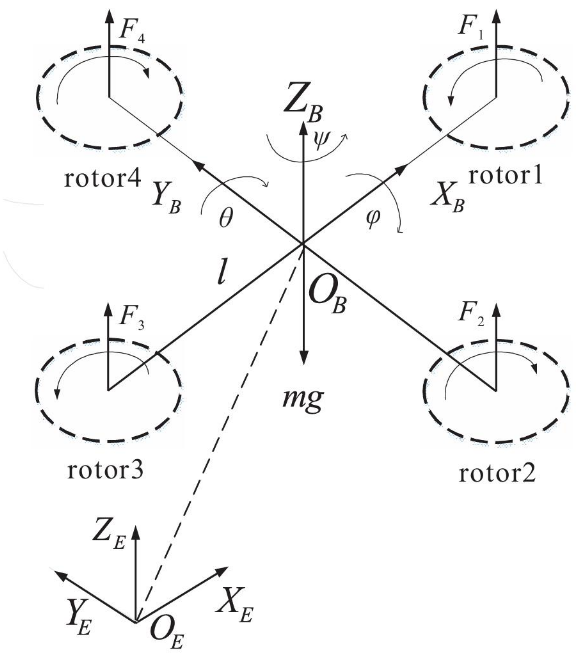

Fig. 1. Schematic Diagram of Inertial Coordinate System and Body Coordinate System.

The nonlinear mathematical model of quadcopter aircraft can be simplified as (Chaoraingern et al., 2020; Jing et al., 2022)

$$\begin{cases} m\ddot{x} = (\cos\phi\sin\theta\cos\psi + \sin\phi\sin\psi)u_1 \\ m\ddot{y} = (\cos\phi\sin\theta\cos\psi + \sin\phi\sin\psi)u_1 \\ m\ddot{z} = (\cos\phi\sin\theta)u_1 - mg \\ J_x\ddot{\phi} = lu_2 + \dot{\theta}\dot{\psi}(J_y - J_z) \\ J_y\ddot{\theta} = lu_3 + \dot{\phi}\dot{\psi}(J_z - J_x) \\ J_z\ddot{\psi} = lu_4 + \dot{\theta}\dot{\phi}(J_x - J_y) \end{cases} \tag{6}$$

where the variables (x, y, z) and (ϕ, θ, ψ) represent the position coordinates and attitude information of the aerial vehicle, respectively. The mass of the vehicle is denoted by m , and l signifies the distance from the center of the propeller to the center of the vehicle. The moments of inertia about the x, y, and z axes are represented by J_x,J_y and J_z, respectively. The control inputs for the model are denoted by $u_i(i = 1, 2, 3, 4)$.

For the convenience of controller design, the mathematical model is constructed in the following form:

$$\begin{cases} x_1 = \phi \\ x_2 = \dot{\phi} = \dot{x}_1 \\ x_3 = \theta \\ x_4 = \dot{\theta} = \dot{x}_3 \\ x_5 = \psi \\ x_6 = \dot{\psi} = \dot{x}_5 \\ x_7 = z \\ x_8 = \dot{z} = \dot{x}_7 \\ x_9 = x \\ x_{10} = \dot{x} = \dot{x}_9 \\ x_{11} = y \\ x_{12} = \dot{y} = \dot{x}_{11} \end{cases} \tag{7}$$

Equation (6) can be split into a rotational subsystem S for attitude control and a translational subsystem S for position control, that is

$$S1: \begin{cases} \dot{x}_1 = x_2 \\ \dot{x}_2 = x_4x_6a_1 + b_1u_2 \\ \dot{x}_3 = x_4 \\ \dot{x}_4 = x_2x_6a_2 + b_2u_3 \\ \dot{x}_5 = x_6 \\ \dot{x}_6 = x_2x_4a_3 + b_3u_4 \end{cases} \tag{8}$$

$$S2: \begin{cases} \dot{x}_7 = x_8 \\ \dot{x}_8 = -g + \cos x_1 \cos x_3 u_1/m \\ \dot{x}_9 = x_{10} \\ \dot{x}_{10} = u_x u_1/m \\ \dot{x}_{11} = x_{12} \\ \dot{x}_{12} = u_y u_1/m \end{cases} \tag{9}$$

where $a_1 = \frac{J_y - J_z}{J_x}$, $a_2 = \frac{J_z - J_x}{J_y}$, $a_3 = \frac{J_x - J_y}{J_z}$, $b_1 = l/J_x$,$b_2 = l/J_y$,$b_3 = l/J_z$, $u_x = \cos x_1 \sin x_3 \cos x_5 + \sin x_1 \sin x_5$, $u_y = \cos x_1 \sin x_3 \cos x_5 - \sin x_1 \cos x_5$.

4. DESIGN OF THE FIXED TIME CONTROLLER BASED ON THE INTEGRAL BACKSTEPPING METHOD

According to equation (6), the research problem of quadcopter control is an underactuated control problem, which will be analyzed in detail below.

4.1 Attitude Control of Quadrotor

From equation (7), it can be seen that in the attitude of a quadcopter aircraft, ϕ, θ and ψ can be controlled by $u_i = (i = 1, 2, 3)$, respectively.

In order to provide readers with a clearer understanding of the entire controller design process, taking the roll angle controller design as an example, we will briefly explain the entire process of designing a fixed time controller (similar to other controller design processes in the paper). Firstly, define the roll angle tracking error; Then, construct a Lyapunov function containing the error, take the derivative of the function, and obtain a dummy variable that satisfies the fixed time stability condition; Finally, define the virtual variable error, construct a Lyapunov function containing virtual variables, and finally obtain the expression of the controller that satisfies the fixed time stability condition.

The flight target trajectory (x_d,y_d,z_d) and yaw angle ψ_d in the actual flight mission are usually known data. The control strategy design process of the aircraft is shown in Figure 2. Firstly, the altitude controller u_1 of the aircraft is designed from the desired altitude of the desired trajectory. The controller u_1 makes the altitude position of the aircraft flight conform to the desired trajectory, and then the virtual controllers u_x and u_y of the horizontal position are obtained by using the relationship between the altitude controller u_1 and the horizontal direction system equation; Then the desired roll angle ϕ_d and the desired pitch angle θ_d of the aircraft are solved by using the inverse solution module; Finally, the attitude position controllers u_2, u_3 and u_4 of the system are designed respectively from the desired roll angle ϕ_d, the desired pitch angle θ_d and the desired yaw angle ψ_d of the aircraft, and the whole controller design process is completed in this order.

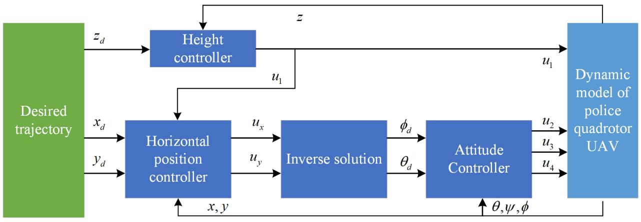

Fig. 2. Control Strategy Chart.

(1) Control of roll angle

Firstly, define the roll angle tracking error as

$$e_\phi = \phi_d - \phi = x_{1d} - x_1 \tag{10}$$

where $\phi_d = x_{1d}$ is the expected roll angle trajectory.

By constructing a Lyapunov function V_3, we have

$$\begin{aligned} V_3 &= V_1 + V_2 \\ &= \frac{1}{2}e_\phi^2 + \frac{1}{2}k_\phi(\int e_\phi dt)^2 \end{aligned} \tag{11}$$

The derivative of equation (10) is

$$\begin{aligned} \dot{V}_3 &= e_\phi \dot{e}_\phi + k_\phi e_\phi \int e_\phi dt \\ &= e_\phi(\dot{x}_{1d} - \dot{x}_1) + k_\phi e_\phi \int e_\phi dt \end{aligned} \tag{12}$$

In order to satisfy the fixed time lemma, we have

$$\begin{aligned} e_\phi(\dot{x}_{1d} - \dot{x}_1) + k_\phi e_\phi \int e_\phi dt &= -sgn(e_\phi) - e_\phi^4 \\ &\quad - sgn(\int e_\phi dt) - (\int e_\phi dt)^4 \\ &= -V_1^{1/2} - V_1^2 - V_2^{1/2} - V_2^2 \end{aligned} \tag{13}$$

If $\dot{x}_1$ is treated as a virtual control variable, then when the expected virtual control is $\alpha_1 = (\dot{x}_1)_d$, it is as follows

$$\begin{aligned} \alpha_1 &= \dot{x}_{1d} + (sgn(e_\phi) + e_\phi^4 + sgn(\int e_\phi dt) \\ &+ (\int e_\phi dt)^4 + k_\phi e_\phi \int e_\phi dt)/e_\phi \end{aligned} \tag{14}$$

We can obtain the following equation:

$$\dot{V}_3 = -V_1^{1/2} - V_1^2 - V_2^{1/2} - V_2^2 \tag{15}$$

Therefore, the error of the virtual control variable $\dot{x}_1$ is defined as

$$e_{\phi 1} = \alpha_1 - \dot{x}_1 \tag{16}$$

By differentiating the aforementioned equation, we can derive

$$\dot{e}_{\phi 1} = \dot{\alpha}_1 - \ddot{x}_1 = \dot{\alpha}_1 - x_4 x_6 a_1 - b_1 u_2 \tag{17}$$

By constructing a Lyapunov function V_5, we have

$$V_5 = V_3 + V_4 \tag{18}$$

where $V_4 = \frac{1}{2}e_{\phi_1}^2$.

By differentiating equation (17), we can arrive at

$$\begin{aligned} \dot{V}_5 &= \dot{V}_3 + \dot{V}_4 \\ &= e_\phi \dot{e}_\phi + k_\phi e_\phi \int e_\phi dt + e_{\phi_1}\dot{e}_{\phi_1} \\ &= e_\phi \dot{e}_\phi + k_\phi e_\phi \int e_\phi dt + e_{\phi_1}(\dot{\alpha}_1 - x_4 x_6 a_1 - b_1 u_2) \end{aligned} \tag{19}$$

In order to satisfy the fixed time lemma, we have

$$\dot{\alpha}_1 - x_4 x_6 a_1 - b_1 u_2 = -\mathrm{sgn}(e_{\phi_1})/e_{\phi_1} - e_{\phi_1}^3 \tag{20}$$

At this point, u_2 satisfies the following equation

$$\dot{\alpha}_1 - x_4 x_6 a_1 - b_1 u_2 = -\mathrm{sgn}(e_{\phi_1})/e_{\phi_1} - e_{\phi_1}^3 \tag{21}$$

We can obtain the expression for u_2 as

$$u_2 = (\mathrm{sgn}(e_{\phi_1})/e_{\phi_1} + e_{\phi_1}^3 - \dot{\alpha}_1 + x_4 x_6 a_1)/b_1 \tag{22}$$

By differentiating V_4 and substituting u_2 within, we have

$$\dot{V}_4 = e_{\phi_1}\dot{e}_{\phi_1} = -sgn(e_{\phi_1}) - e_{\phi_1}^4 \tag{23}$$

According to Lemma 2, it can be concluded that

$$\begin{aligned} \dot{V}_3 &= -V_1^{1/2} - V_1^2 - V_2^{1/2} - V_2^2 - V_3^{1/2} - V_3^2 \\ &<= -(V_1 + V_2 + V_3)^{1/2} - -(V_1 + V_2 + V_3)^2 \end{aligned} \tag{24}$$

(2) Control of pitch angle

The control mechanism of pitch angle is similar to that of roll angle. Firstly, the pitch angle tracking error angle is defined as

$$e_\theta = \theta_d - \theta = x_{3d} - x_3 \tag{25}$$

where x_{3d} is the expected pitch angle trajectory.

Constructing a Lyapunov function V_8 as

$$\begin{aligned} V_8 &= V_6 + V_7 \\ &= \tfrac{1}{2}e_\theta^2 + \tfrac{1}{2}k_\theta(\textstyle\int e_\theta dt)^2 \end{aligned} \tag{26}$$

The derivative of equation (25) is

$$\begin{aligned} \dot{V}_8 &= e_\theta \dot{e}_\theta + k_\theta e_\theta \textstyle\int e_\theta dt \\ &= e_\theta(\dot{x}_{3d} - \dot{x}_3) + k_\theta e_\theta \textstyle\int e_\theta dt \end{aligned} \tag{27}$$

In order to satisfy the fixed time lemma, we have

$$\begin{aligned} e_\theta(\dot{x}_{3d} - \dot{x}_3) + k_\theta e_\theta \int e_\theta dt &= -sgn(e_\theta) - e_\theta^4 \\ &\quad - sgn(\int e_\theta dt) - (\int e_\theta dt)^4 \\ &= -V_6^{1/2} - V_6^2 - V_7^{1/2} - V_7^2 \end{aligned} \tag{28}$$

If $\dot{x}_3$ is treated as a virtual control variable, then when the expected virtual control is $\alpha_2 = (\dot{x}_3)_d$, it is as follows

$$\begin{aligned} \alpha_2 &= \dot{x}_{3d} + (sgn(e_\theta) + e_\theta^4 + sgn(\int e_\theta dt) \\ &+ (\int e_\theta dt)^4 + k_\theta e_\theta \int e_\theta dt)/e_\theta \end{aligned} \tag{29}$$

We can obtain the following equation:

$$\dot{V}_8 = -V_6^{1/2} - V_6^2 - V_7^{1/2} - V_7^2 \tag{30}$$

Therefore, the error of the virtual control variable $\dot{x}_3$ is defined as

$$e_{\theta 1} = \alpha_2 - \dot{x}_3 \tag{31}$$

By differentiating the above equation, we have

$$\dot{e}_{\theta 1} = \dot{\alpha}_2 - \ddot{x}_3 = \dot{\alpha}_2 - x_2 x_6 a_2 - b_2 u_3 \quad (32)$$

By constructing a Lyapunov function V_{10}, we have

$$V_{10} = V_8 + V_9 \quad (33)$$

where $V_9 = \frac{1}{2} e_{\theta 1}^2$.

In order to satisfy the fixed time lemma, we have

$$\dot{\alpha}_2 - x_2 x_6 a_2 - b_2 u_3 = -\mathrm{sgn}(e_{\theta 1})/e_{\theta 1} - e_{\theta 1}^3 \quad (34)$$

We can obtain the expression for u_3 as

$$u_3 = (\mathrm{sgn}(e_{\theta 1})/e_{\theta 1} + e_{\theta 1}^3 + \dot{\alpha}_2 - x_2 x_6 a_2)/b_2 \quad (35)$$

By differentiating V_9 and substituting u_3 within, we can obtain

$$\dot{V}_9 = e_{\theta_1} \dot{e}_{\theta_1} = -sgn(e_{\phi_1}) - e_{\phi_1}^4 \quad (36)$$

According to Lemma 2, it can be concluded that

$$\begin{aligned} \dot{V}_{10} &= -V_6^{1/2} - V_6^2 - V_7^{1/2} - V_7^2 - V_9^{1/2} - V_9^2 \\ &<= -(V_6 + V_7 + V_9)^{1/2} - -(V_6 + V_7 + V_9)^2 \end{aligned} \quad (37)$$

(3) Control of yaw angle

Firstly, define the yaw angle tracking error angle as

$$e_\psi = \psi_d - \psi = x_{5d} - x_5 \quad (38)$$

where x_{5d} is the expected pitch angle trajectory.

By constructing a Lyapunov function V_{13} ,we have

$$\begin{aligned} V_{13} &= V_{11} + V_{12} \\ &= \frac{1}{2} e_\psi^2 + \frac{1}{2} k_\psi (\int e_\psi dt)^2 \end{aligned} \quad (39)$$

The derivative of equation (13) is

$$\begin{aligned} \dot{V}_{13} &= e_\psi \dot{e}_\psi + k_\psi e_\psi \int e_\psi dt \\ &= e_\psi (\dot{x}_{5d} - \dot{x}_5) + k_\psi e_\psi \int e_\psi dt \end{aligned} \quad (40)$$

In order to satisfy the fixed time lemma, we have

$$\begin{aligned} e_\psi (\dot{x}_{5d} - \dot{x}_5) + k_\psi e_\psi \int e_\psi dt &= -sgn(e_\psi) - e_\psi^4 \\ &- sgn(\int e_\psi dt) - (\int e_\psi dt)^4 \\ &= -V_{11}^{1/2} - V_{11}^2 - V_{12}^{1/2} - V_{12}^2 \end{aligned} \quad (41)$$

If $\dot{x}_5$ is treated as a virtual control variable, then when the expected virtual control is $\alpha_3 = (\dot{x}_5)_d$, it is as follows

$$\begin{aligned} \alpha_3 &= \dot{x}_{5d} + (sgn(e_\psi) + e_\psi^4 + sgn(\int e_\psi dt) \\ &+ (\int e_\psi dt)^4 + k_\psi e_\psi \int e_\psi dt)/e_\psi \end{aligned} \quad (42)$$

We can obtain the following equation:

$$\dot{V}_{13} = -V_{11}^{1/2} - V_{11}^2 - V_{12}^{1/2} - V_{12}^2 \quad (43)$$

Therefore, the error of the virtual control variable $\dot{x}_3$ is defined as

$$e_{\psi 1} = \alpha_3 - \dot{x}_5 \quad (44)$$

By differentiating the above equation, we have

$$\dot{e}_{\psi 1} = \dot{\alpha}_3 - \ddot{x}_5 = \dot{\alpha}_3 - x_2 x_4 a_3 - b_3 u_4 \quad (45)$$

By constructing a Lyapunov function V_{15}, we have

$$V_{15} = V_{13} + V_{14} \quad (46)$$

where $V_{14} = \frac{1}{2} e_{\psi 1}^2$.

In order to satisfy the fixed time lemma, we have

$$\dot{\alpha}_3 - x_2 x_4 a_3 - b_3 u_4 = -\mathrm{sgn}(e_{\psi 1})/e_{\psi 1} - e_{\psi 1}^3 \quad (47)$$

We can obtain the expression for u_4 as

$$u_4 = (\mathrm{sgn}(e_{\psi 1})/e_{\psi 1} + e_{\psi 1}^3 + \dot{\alpha}_3 - x_2 x_4 a_3)/b_3 \quad (48)$$

By differentiating V_{14} and substituting u_4 with, we can obtain

$$\dot{V}_{14} = e_{\theta_1} \dot{e}_{\theta_1} = -sgn(e_{\phi_1}) - e_{\phi_1}^4 \quad (49)$$

According to Lemma 2, it can be concluded that

$$\begin{aligned} \dot{V}_{15} &= -V_{11}^{1/2} - V_{11}^2 - V_{12}^{1/2} - V_{12}^2 - V_{14}^{1/2} - V_{14}^2 \\ &<= -(V_{11} + V_{12} + V_{14})^{1/2} - -(V_{11} + V_{12} + V_{14})^2 \end{aligned} \quad (50)$$

4.2 Position Control of Quadrotor

From equations (5) and (8), it can be seen that the two degrees of freedom of the horizontal coordinates x and y are underactuated, indirectly driven by ϕ, θ, and ψ, respectively.

(1) Tracking control of height position

Regarding height control, this article also adopts the integral backstepping method. Define the height tracking error as

$$e_{z1} = z_d - z = x_{7d} - x_7 \quad (51)$$

where x_{7d} is the expected altitude trajectory.

By constructing a Lyapunov function V_{18} ,we have

$$\begin{aligned} V_{18} &= V_{16} + V_{17} \\ &= \frac{1}{2} e_{z1}^2 + \frac{1}{2} k_{z1} (\int e_{z1} dt)^2 \end{aligned} \quad (52)$$

The derivative of equation (51) is

$$\begin{aligned} \dot{V}_{18} &= e_{z1} \dot{e}_{z1} + k_{z1} e_{z1} \int e_{z1} dt \\ &= e_{z1} (\dot{x}_{7d} - \dot{x}_7) + k_{z1} e_{z1} \int e_{z1} dt \end{aligned} \quad (53)$$

In order to satisfy the fixed time lemma, we have

$$\begin{aligned} e_{z1} (\dot{x}_{7d} - \dot{x}_7) + k_{z1} e_{z1} \int e_{z1} dt &= -sgn(e_{z1}) - e_{z1}^4 \\ &- sgn(\int e_{z1} dt) - (\int e_{z1} dt)^4 \\ &= -V_{16}^{1/2} - V_{16}^2 - V_{17}^{1/2} - V_{17}^2 \end{aligned} \quad (54)$$

If $\dot{x}_7$ is treated as a virtual control variable, then when the expected virtual control is $\alpha_4 = (\dot{x}_7)_d$, it is as follows

$$\begin{aligned} \alpha_4 &= \dot{x}_{7d} + (sgn(e_{z1}) + e_{z1}^4 + sgn(\int e_{z1} dt) \\ &+ (\int e_{z1} dt)^4 + k_{z1} e_{z1} \int e_{z1} dt)/e_{z1} \end{aligned} \quad (55)$$

We can obtain the following equation:

$$\dot{V}_{18} = -V_{16}^{1/2} - V_{16}^2 - V_{17}^{1/2} - V_{17}^2 \quad (56)$$

Therefore, the error of the virtual control variable $\dot{x}_7$ is defined as

$$e_{z2} = \alpha_4 - \dot{x}_7 \tag{57}$$

By differentiating the above equation, we have

$$\dot{e}_{z2} = \dot{\alpha}_4 - \ddot{x}_7 = \dot{\alpha}_4 + g - \cos x_1 \cos x_3 u_1/m \tag{58}$$

By constructing a Lyapunov function V_{20}, we have

$$V_{20} = V_{18} + V_{19} \tag{59}$$

where $V_{19} = \frac{1}{2}e_{z2}^2$.

In order to satisfy the fixed time lemma, we have

$$\dot{\alpha}_4 + g - \cos x_1 \cos x_3 u_1/m = -\mathrm{sgn}(e_{z2})/e_{z2} - e_{z2}^3 \tag{60}$$

We can obtain the expression for u_1 as

$$u_1 = (\dot{\alpha}_4 + g + \mathrm{sgn}(e_{z2})/e_{z2} + e_{z2}^3)m/(\cos x_1 \cos x_3) \tag{61}$$

By differentiating V_{19} and substituting u_1 within, we have

$$\dot{V}_{19} = e_{z2}\dot{e}_{z2} = -sgn(e_{z2}) - e_{z2}^4 \tag{62}$$

According to Lemma 2, it can be concluded that

$$\begin{aligned}\dot{V}_{20} &= -V_{16}^{1/2} - V_{16}^2 - V_{17}^{1/2} - V_{17}^2 - V_{19}^{1/2} - V_{19}^2 \\ &<= -(V_{16} + V_{17} + V_{19})^{1/2} - (V_{16} + V_{17} + V_{19})^2\end{aligned} \tag{63}$$

(2) Control of horizontal position

Define the horizontal position tracking error as

$$e_{x1} = x_d - x = x_{9d} - x_9 \tag{64}$$

where x_{9d} is the expected altitude trajectory.

By constructing a Lyapunov function V_{23}, we have

$$\begin{aligned}V_{23} &= V_{21} + V_{22} \\ &= \frac{1}{2}e_{x1}^2 + \frac{1}{2}k_{x1}(\int e_{x1}dt)^2\end{aligned} \tag{65}$$

The derivative of equation (64) is

$$\begin{aligned}\dot{V}_{23} &= e_{x1}\dot{e}_{x1} + k_{x1}e_{x1}\int e_{x1}dt \\ &= e_{x1}(\dot{x}_{9d} - \dot{x}_9) + k_{x1}e_{x1}\int e_{x1}dt\end{aligned} \tag{66}$$

In order to satisfy the fixed time lemma, we have

$$\begin{aligned}e_{x1}(\dot{x}_{9d} - \dot{x}_9) + k_{x1}e_{x1}\int e_{x1}dt &= -sgn(e_{x1}) - e_{x1}^4 \\ &- sgn(\int e_{x1}dt) - (\int e_{x1}dt)^4 \\ &= -V_{21}^{1/2} - V_{21}^2 - V_{22}^{1/2} - V_{22}^2\end{aligned} \tag{67}$$

If $\dot{x}_9$ is treated as a virtual control variable, then when the expected virtual control is $\alpha_5 = (\dot{x}_9)_d$, it is as follows

$$\begin{aligned}\alpha_5 = \dot{x}_{9d} &+ (sgn(e_{x1}) + e_{x1}^4 + sgn(\int e_{x1}dt) \\ &+ (\int e_{x1}dt)^4 + k_{x1}e_{x1}\int e_{x1}dt)/e_{x1}\end{aligned} \tag{68}$$

We can obtain the following equation:

$$\dot{V}_{23} = -V_{21}^{1/2} - V_{21}^2 - V_{22}^{1/2} - V_{22}^2 \tag{69}$$

Therefore, the error of the virtual control variable $\dot{x}_9$ is defined as

$$e_{x2} = \alpha_5 - \dot{x}_9 \tag{70}$$

By differentiating the above equation, we can obtain

$$\dot{e}_{x2} = \dot{\alpha}_5 - \ddot{x}_9 = \dot{\alpha}_4 - u_x u_1/m \tag{71}$$

By constructing a Lyapunov function V_{25}, we have

$$V_{25} = V_{23} + V_{24} \tag{72}$$

where $V_{24} = \frac{1}{2}e_{x2}^2$.

In order to satisfy the fixed time lemma, we have

$$\dot{\alpha}_5 - u_x u_1/m = -\mathrm{sgn}(e_{x2})/e_{x2} - e_{x2}^3 \tag{73}$$

We can obtain the expression for u_x as

$$u_x = (\dot{\alpha}_5 + \mathrm{sgn}(e_{x2})/e_{x2} + e_{x2}^3)m/u_1 \tag{74}$$

By differentiating V_{24} and substituting u_x within, we can obtain

$$\dot{V}_{24} = e_{x2}\dot{e}_{x2} = -sgn(e_{x2}) - e_{x2}^4 \tag{75}$$

According to Lemma 2, it can be concluded that

$$\begin{aligned}\dot{V}_{25} &= -V_{21}^{1/2} - V_{21}^2 - V_{22}^{1/2} - V_{22}^2 - V_{24}^{1/2} - V_{24}^2 \\ &<= -(V_{21} + V_{22} + V_{24})^{1/2} - (V_{21} + V_{22} + V_{24})^2\end{aligned} \tag{76}$$

Using the same method, the expression for u_y can be obtained as follows

$$u_y = (\dot{\alpha}_6 + \mathrm{sgn}(e_{y2})/e_{y2} + e_{y2}^3)m/u_1 \tag{77}$$

The expressions for the expected trajectory of roll angle and pitch angle can be obtained from equation (8):

$$\begin{cases}\phi_d = \arcsin(u_x \sin x_5 - u_y \cos x_5) \\ \theta_d = \arcsin\left(u_y/(\cos\phi_d \sin x_5) + (\sin\phi_d \cos x_5)/(\cos\phi_d \sin x_5)\right)\end{cases} \tag{78}$$

The aforementioned process has meticulously concluded the design of fixed-time controllers specifically tailored to regulate the aircraft's angle, position, and altitude. This intricate and comprehensive design is grounded in the principles of fixed-time control theory, seamlessly integrating the advanced integral backstepping method. Consequently, the controllers, owing to this meticulous design, ensure unparalleled precision and timing in controlling the diverse flight parameters of the aircraft.

Consequently, this ensures a significant improvement in the aircraft's overall performance and stability throughout its flight operations, ultimately contributing to a safer and more efficient flying experience.

4.3 Overall control process

Based on the above analysis, which details the mathematical formulation and implementation steps, the overall control process of a quadcopter aircraft utilizing the integral backstepping method is comprehensively illustrated in Figure 3. This figure depicts the various stages and components involved in the control system, showcasing how the integral backstepping technique ensures stability and performance of the quadcopter during flight operations

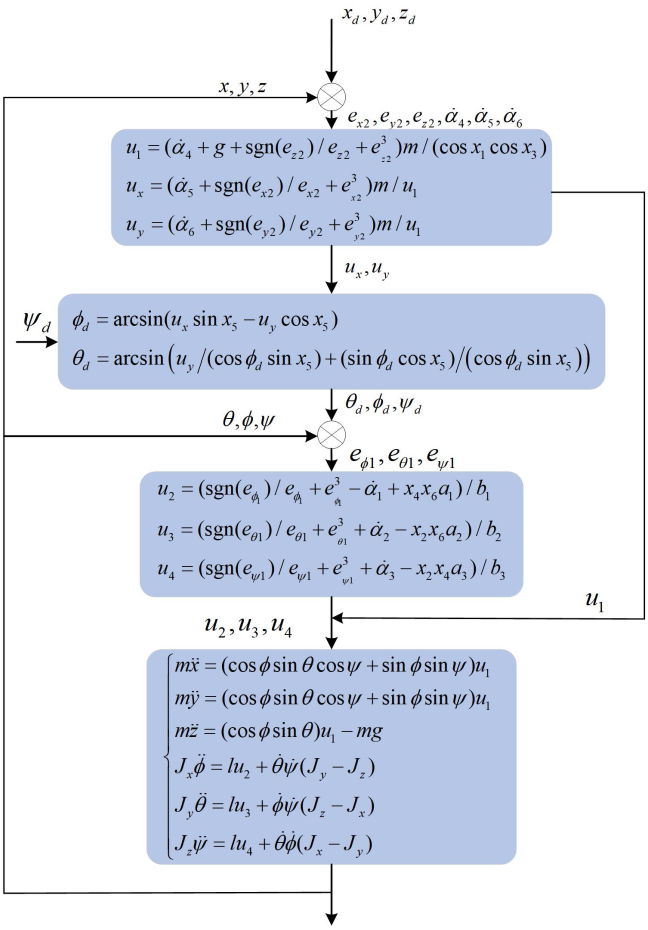

Fig. 3. Control Flowchart of the Proposed Method.

5. SIMULATION RESULTS AND ANALYSIS

The main parameters of the aircraft are as follows

Table 1. Main parameters of quadcopter aircraft

Parameter	m(kg)	$J_x(kg \cdot m^2)$	$J_y(kg \cdot m^2)$	$J_z(kg \cdot m^2)$	l(m)
value	0.265	0.0104	0.0104	0.0208	0.0103

In order to demonstrate the design effect of a fixed time controller for quadcopter aircraft based on integral backstepping method, comparisons were made with PID controller and sliding mode controller. The required tracking trajectory is designed as a spiral ascent process, with a simulation time of 100 s, position height unit in m, and angle unit in deg. The specific mathematical equation is:

$$\begin{cases} \psi_d = 0 \\ x_d = 8\sin(0.2t) \\ y_d = 8\sin(0.2t + \frac{\pi}{2}) \\ z_d = -8 + 0.2t \end{cases} \tag{79}$$

1) Fixed time controller for quadcopter aircraft based on integral backstepping method

As shown in Fig. 4, it can be seen from the 3D tracking image that the quadcopter perfectly tracked the target trajectory (including angle and position), and the aircraft can also quickly track during the spiral upward change of the trajectory.

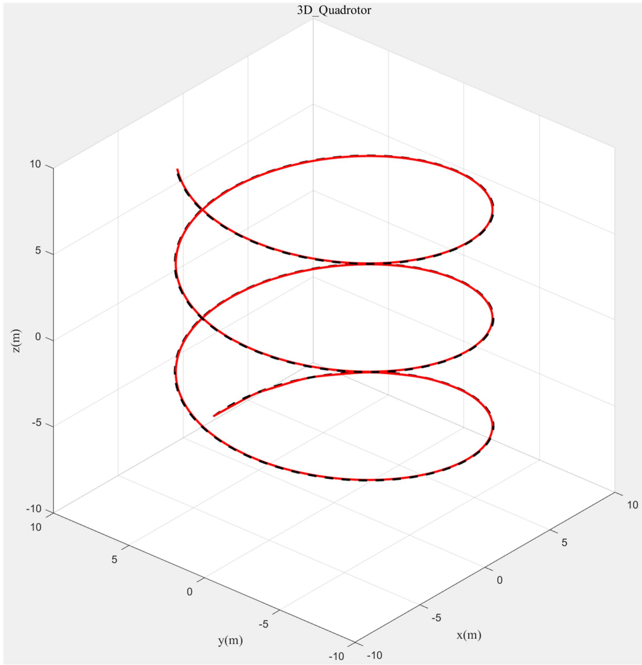

Fig. 4. 3D Tracking Image with Proposed Controller.

Fig. 5 specifically shows the error changes of x, y, z, yaw angle. It is observable that the errors in the x direction are all within 0.10 m, and the errors in the y direction are all within 0.04 m. The error in the yaw angle can be ignored. From the figure, it is observable that x, y, x, yaw angle can quickly and accurately converge to the desired target value without steady-state error under the action of the proposed controller in a short period of time. As shown in Fig. 4, it can be seen that the quadcopter perfectly tracks the target trajectory (including angle and position), and the aircraft can also quickly track during the spiral upward change of the trajectory. Fig. 5 specifically shows the tracking effect of position height x, y, z and angle ϕ, θ, ψ. It is observable that the proposed controller can accurately track the target trajectory in terms of position and height. Pitch angle can accurately and quickly track to the reference angle. Roll angle and yaw angle can also accurately track the changes in actual angle values, with an error within 2 deg in Fig. 6.

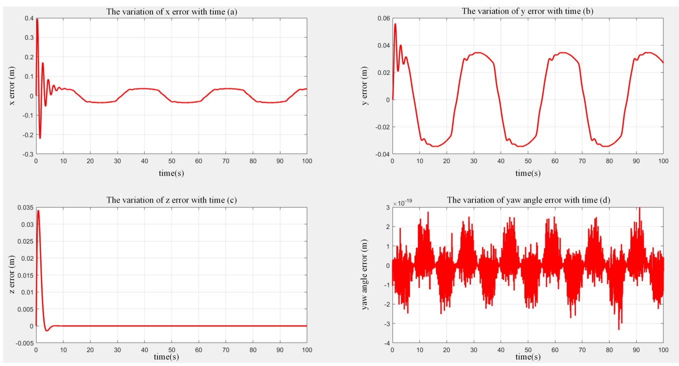

Fig. 5. Error Plot of X, Y, Z, and Yaw angle under the Proposed Controller.

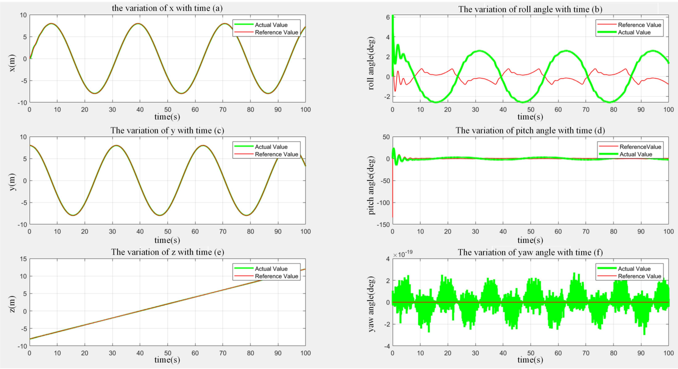

Fig. 6. Tracking Curves of X, Y, Z Directions and Angles under the Proposed Controller.

2) Simulation of quadcopter aircraft based on PID controller

The simulation results are shown in Fig. 7. From the 3D tracking map, it is observable that the quadcopter can also track the target trajectory (including angle and position), and during the spiral upward change of the trajectory, the aircraft can also quickly track, but there is a significant error compared to the tracking effect of the proposed controller.

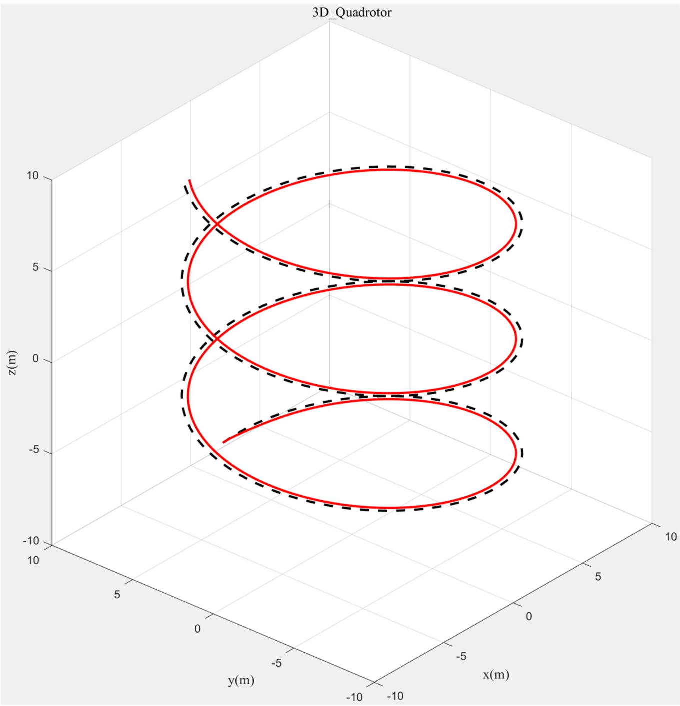

Fig. 7. 3D Tracking Image with PID Controller.

Fig. 8 specifically shows the error variation of x, y, z, yaw angle. It is observable that the errors in both the x and y directions are within 0.21 m, and the error in yaw angle is around 0.20 deg. From the figure, it is observable that x, y, z, yaw angle can all converge to the desired target value under the action of the PID controller, but there is a significant steady-state error compared to the proposed controller. As shown in Fig. 7, it can be seen that the quadcopter tracked the target trajectory (including angle and position) under the action of the PID controller, but the tracking effect error was significant. Fig. 7 specifically shows the tracking effect of position height x, y, z and angle ϕ, θ, ψ. It can be seen that the proposed controller can accurately track the target trajectory in terms of position and height. Pitch angle and yaw angle can quickly track to the reference angle. The tracking effect of roll angle is poor, with a 6 deg error in Fig. 9.

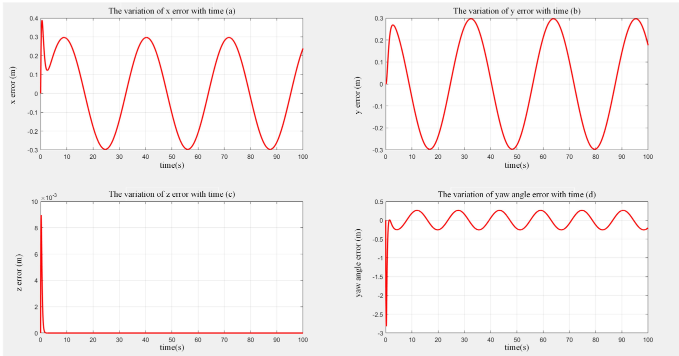

Fig. 8. Error Plot of X, Y, Z, and Yaw angle under the PID Controller.

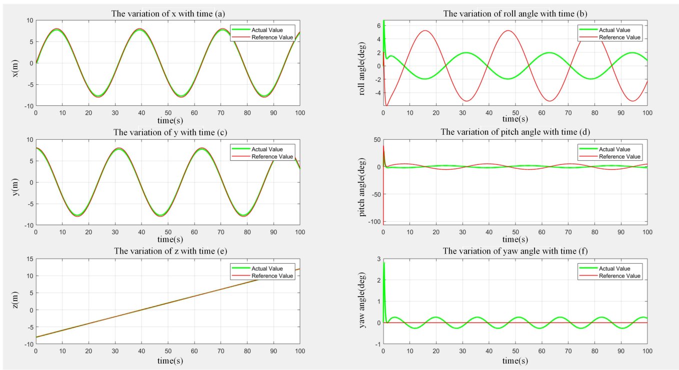

Fig. 9. Tracking Curves of X, Y, Z Directions and Angles under the PID Controller.

3) Simulation based on sliding mode controller

As shown in Fig. 10, from the 3D tracking image, it is observable that the quadcopter can achieve tracking of the target trajectory (including angle and position), and during the spiral upward change of the trajectory, the aircraft also moves along the target trajectory.

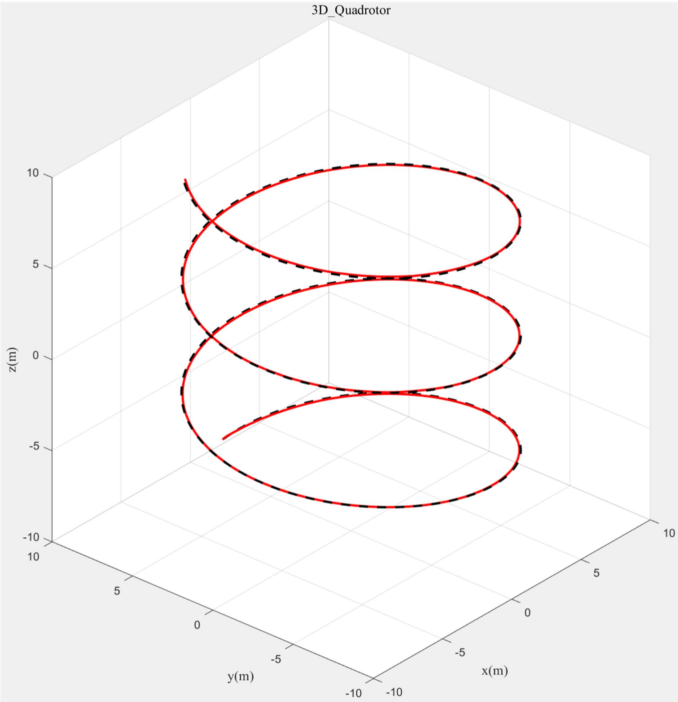

Fig. 10. 3D Tracking Image with Sliding Mode Controller.

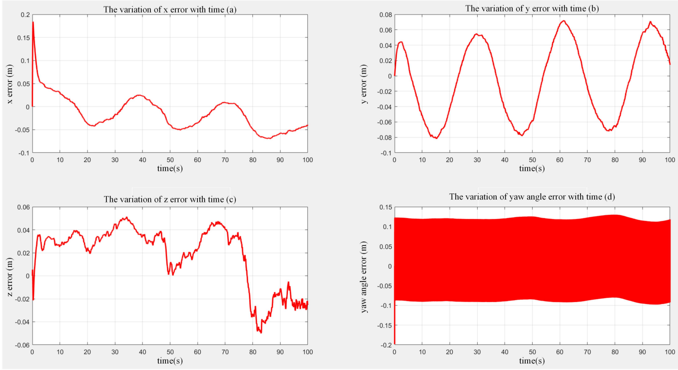

Fig. 11. Error Plot of X, Y, Z, and Yaw angle under the Sliding Mode Controller.

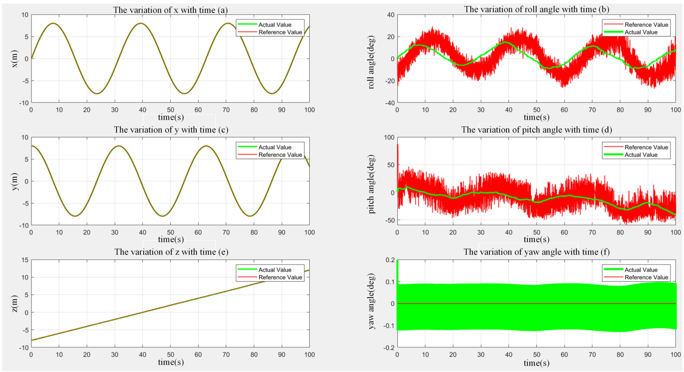

Fig. 12. Tracking Curves of X, Y, Z Directions and Angles under the Sliding Mode Controller.

Fig. 11 specifically shows the error variation of x, y, x, yaw angle. It can be seen that the errors in the x and y directions are within 0.98 m, and the error in the yaw angle is around 0.11 deg. From the figure, it is observable that x, y, x, yaw angle can converge to the desired target value with minimal error under the action of the sliding mode controller, but there is still a gap compared to the proposed controller. As shown in the 3D tracking image, it is observable that the quadcopter can track the target trajectory (including angle and position). Fig. 12 specifically shows the tracking effect of position height x, y, z and angle ϕ, θ, ψ. It can be seen that the proposed controller can accurately track the target trajectory in terms of position and height, but there is a significant error in angle, with a pitch angle error of about 30 deg. The roll angle error is around 15 deg, and the yaw angle can accurately track changes in the actual angle value, with an error within 0.1 deg. Table 2 also shows that compared with PID method and sliding mode method, the error of x, y, z and yaw angle error of the proposed algorithm are the smallest.

Table 2. Comparison of position and yaw angle errors under three algorithms

Method	X- Error	Y- Error	Z- Error	Yaw angle-Error
PID method	0.30	0.31	0.005	0.35
Sliding mode method	0.067	0.082	0.051	0.11
Proposed method	0.032	0.035	0.002	0

4) Design of fixed time controller for quadcopter aircraft based on integral backstepping method and comparison with the effect without integral term

Taking fixed-point tracking of 1m in the x-direction as an example, as shown in Fig. 13, it is observable that both can accurately track the position of 1m. The difference is that the simplified controller of the control model reduces the control force by adjusting the integral term parameters, and its convergence time (7.4s) is slightly longer than the convergence time before the simplification of the control model (3.4s).

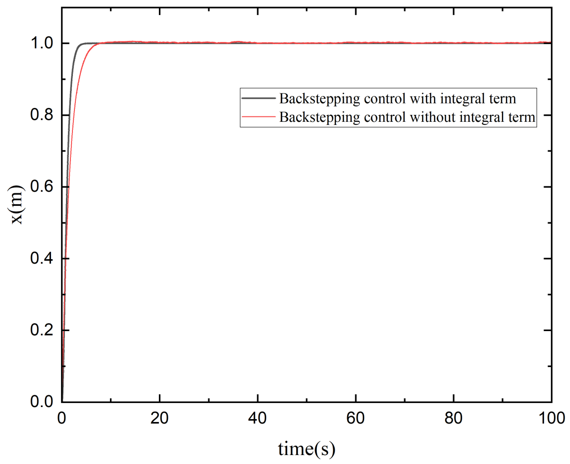

Fig. 13. Comparison of X-tracking Curves with and without Integral Terms.

The table also shows the computation time of each step of the quadcopter aircraft under the action of various attitude controllers before and after simplification, as shown in Table 3. It is observable that the operation time of each step of the control model is shorter after simplification using the integral term. Figure 13 and Table 3 demonstrate that the proposed approach of simplifying the attitude control model by adjusting the integral term parameters is feasible, and has high significance for applying it to simulation experiments of aircraft fixed-point arrival and trajectory tracking.

Table 3. Comparison of single step running time with and without integral terms

Controller	Average single step running time(ms)
With integral terms	0.02869
Without integral terms	0.05933

The above simulation results strongly demonstrate the effectiveness of the proposed controller. However, the limitations of controller design need to be recognized. In reality, there is noise in sensors or inevitable wind disturbance to drones, causing them to deviate from the expected trajectory. In this case, certain improvements can be made in the original design scheme. If interference terms are introduced in the position altitude and attitude angle during flight, of course, these interferences are bounded external interference terms. At this point, it is only necessary to construct the expression of the disturbance term error using the same method. When constructing the Lyapunov function, the disturbance error energy function is introduced to obtain the update rate of the disturbance estimation value that satisfies the fixed time control lemma. There is also a problem of computational complexity in the real world. When the calculation process of the controller is complex, the computational load is enormous. At this time, it is necessary to optimize the calculation process, such as adding instruction filters, and designing a lightweight model of the controller to run on embedded device platforms. This is also a meaningful research direction for the future.

6. CONCLUSIONS

This paper proposes a fixed time controller for police quadcopter aircraft based on integral backstepping method. In the control design process, an integral term is introduced in the backstepping design of attitude control. By setting appropriate integral term constants, the controller model is simplified, the practicality of the algorithm is enhanced, and the running time of the model was shortened. In order to solve the problem of slow system tracking response, a fast and stable aircraft controller is constructed by combining backstepping method and fixed time control. Compared with PID control, the proposed algorithm reduces x-direction error by 50% and y-direction error by 80%. Compared with sliding mode control, the x-direction error is reduced by 2% and the y-direction error is reduced by 60%. The yaw angle error under the proposed control algorithm is almost zero.Compared with the backstepping controller without an integral term, the proposed algorithm reduces the single step running time by 51.6%. The simulation results show that compared with PID and sliding mode control, the controller can quickly and stably achieve trajectory tracking.

The significance of this paper is to explore the application of fixed time control based on integral backstepping method in quadcopter police unmanned aerial vehicles.This article can summarize some conclusions. Firstly, in the improved algorithm, introducing an integral term can simplify the algorithm and shorten the model running time. Secondly, the introduction of a fixed time control strategy can improve the speed of trajectory tracking in the system. This provides a foundation for the application of the algorithm in practical environments. However, it is worth noting that the proposed algorithm has a strong dependence on model accuracy, which can complicate stability proofs in the presence of high-frequency noise or communication delays. In the future, the focus will be on combining fixed time control with lightweight deployment of drones, and building an open-source drone testing platform with unified evaluation indicators to improve the real-time performance of algorithms.

REFERENCES

Ahn, H., Hu, M., Chung, Y. (2023). Sliding-mode control for flight stability of quadrotor drone using adaptive super-twisting reaching law. *Drones*, 7(8), 522.

Amertet, S., Gebresenbet, G., & Alwan, H. (2024). Modeling of unmanned aerial vehicles for smart agriculture systems using hybrid fuzzy PID controllers. *Applied Sciences* , 14(8), pp. 34-58.

Askarzadeh, T., Bridgelalt, R., & Tolliver, D. (2023). Systematic literature review of drone utility in railway condition monitoring. *Transportation Engineering, Part A: Systems*, 149(6), 04023041.

Belmouhoub, A., Medjmadj, S., Bouzid, Y. (2023). Enhanced backstepping control for an unconventional quadrotor under external disturbances. *The Aeronautical Journal*, 127(1310), pp. 627-650.

Chaoraingern, J., & Tipsuwanporn, V. (2020). Modified adaptive sliding mode control for trajectory tracking of mini-drone quadcopter unmanned aerial vehicle. *International Journal of Intelligent Engineering and Systems*, 13(5), pp. 145-158.

Cheng, X., Liu, W., Hou, H. (2022). Disturbance observer-based nonsingular fixed-time sliding mode tracking control for a quadcopter. *Science China Information Sciences* , 65(9), pp. 220-231.

Derrouaoui, S., Bouzid, Y., & Guiatni, M. (2022). Adaptive integral backstepping control of a reconfigurable quadrotor with variable parameters? estimation. *Proceedings of the Institution of Mechanical Engineers, Part I: Journal of Systems and Control Engineering*, 236(7), pp. 1294-1309.

Eliker, K., Grouni, S., Tadde, M. (2021). Quadcopter nonsingular finite-time adaptive robust saturated command-filtered control system under the presence of uncertainties and input saturation. *Nonlinear dynamics*, 104(2), pp. 1363-1387.

Ezhil, V., Sriram, B., Vijay, R. (2022). Investigation on PID controller usage on Unmanned Aerial Vehicle for stability control. *Materials Today: Proceedings*, 66, pp. 1313-1318.

Fox, S. (2019). Policing: Monitoring, investigating and prosecuting drones. *European Journal of Comparative Law and Governance*, 6(1), pp. 78-126.

Ghommam, J., Saad, M., & Wright, S. (2020). Relay manoeuvre based fixed-time synchronized tracking control for UAV transport system. *Aerospace Science and Technology*, 103, 105887.

Jahan, N., Niloy, M., & Silvi, F. (2024). Development of an IoT-based firefighting drone for enhanced safety and efficiency in fire suppression. *Measurement and Control*, 29(4), pp. 833-845.

Jammazi, C. (2021). Some results on finite-time stabilizability: application to triangular control systems. *IMA Journal of Mathematical Control and Information*, 35(3), pp. 877-899.

Jing, Y., Wang, X., & Heredia-Juesas, J. (2022). PX4 simulation results of a quadcopter with a disturbance-observer-based and PSO-optimized sliding mode surface controller. *Drones*, 6(9), 261.

Kangunde, V., Jamisola, J., & Theophilus, K. (2021). A review on drones controlled in real-time. *International journal of dynamics and control*, 9(4), pp. 1832-1846.

Labbadi, M., & Cherkaoui, M. (2021). Robust adaptive global time-varying sliding-mode control for finite-time tracker design of quadrotor drone subjected to Gaussian random parametric uncertainties and disturbances. *International Journal of Control, Automation and Systems*, 19(12), pp. 2213-2223.

Liu, W., Chen, M., & Shi, P. (2022). Fixed-time disturbance observer-based control for quadcopter suspension transportation system. *IEEE Transactions on Circuits and Systems I: Regular Papers*, 69(11), pp. 4632-4642.

Liu, M., Ji, R., & Ge, S. (2021). Adaptive neural control for a tilting quadcopter with finite-time convergence. *Neural Computing and Applications*, 33(23), pp. 15987-16004.

Liu, Q., Zhang, K., Pan, Y. (2024). Path?tracking control of tilting quadrotor UAV based on variable structure sliding mode control method. *International Journal of Aerospace Engineering* , 2024(1), 2570976.

Maghazei, O., Steinmann, M. (2020). Drones in railways: Exploring current applications and future scenarios based on action research. *European Journal of Transport and Infrastructure Research*, 20(3), pp. 87-102.

Ning, B., Han, L., Zuo, Z. (2022). Fixed-time and prescribed-time consensus control of multiagent systems and its applications: A survey of recent trends and methodologies. *IEEE Transactions on Industrial Informatics*, 19(2), pp. 1121-1135.

Smith, S., Pan, Y. (2024). Adaptive observer-based super-twisting sliding mode control for low altitude quadcopter grasping. *IEEE/ASME Transactions on Mechatronics*, 7(8), pp. 2021-2030.

Sartori, D., Quagliotti, F., Rutherford, M. (2021).. Design and development of a backstepping controller autopilot for fixed-wing UAVs. *The Aeronautical Journal*, 125(1294), pp. 2087-2113.

Ullah, S., Khan, Q., Mehmood, A. (2019). Integral backstepping integral sliding mode control of underactuated nonlinear electromechanical systems. *Control Engineering and Applied Informatics*, 21(3), pp. 42-50.

Wang, N., Fu Z., Song, S. (2021). Barrier-Lyapunov-based adaptive fuzzy finite-time tracking of pure-feedback nonlinear systems with constraints. *IEEE Transactions on Fuzzy Systems* , 30(4), pp. 1139-1148.

Wang, Y., Tao, F., & Fu, Z. (2023). Adaptive fuzzy fixed-time dynamic surface control for stochastic nonstrict nonlinear systems with unknown dead-zones. *Journal of the Franklin Institute* , 360(6), pp. 4091-4113.

Zhang, X., Zhang, Y., & Hu, Q. (2023). Fixed-time command-filtered adaptive backsteppping control for a class of uncertain mimo systems. *Control Engineering and Applied Informatics*, 25(4), pp. 3-13.

Zheng, R., Zhu, Q., Huang, S. (2024). Extended state observer-based sliding-mode control for aircraft in tight formation considering wake vortices and uncertainty. *Drones* , 8(4), 165.